46th AIAA/ASME/ASCE/AHS/ASC Structures, Structural Dynamics & Materials Conference
18 - 21 April 2005, Austin, Texas

AIAA 2005-2167

Increasing Design Load and Reducing Weight of Structures by Error Reduction

Erdem Acar [*] and Raphael T. Haftka.[†]
University of Florida, Gainesville, FL, 32611-6250

Bhavani V. Sankar [‡]
Business University of Florida, Gainesville, FL, 32611-6250

and

Xueshi Qiu [§]
South West United Machinery Corporation, China

In this paper we analyze tradeoffs of design load, weight and safety of structures via probabilistic design methodology. We first perform the probabilistic analysis of a sandwich panel used in aerospace structures. We explore the effect of using a more accurate prediction technique for interfacial fracture toughness that combines interfacial fracture toughness with mode-mixity instead of using the traditional model that disregards mode-mixity. We find that the use of this more accurate model allows on average 12% increase in design load. Next, we consider structural failure due to point stress without damage propagation in a representative aircraft structure. We find that reducing errors from 50% to 10% provides up to 24% weight savings.

Nomenclature

C and R	=	Capacity and response of the structure, respectively.
e_C and e_R	=	Error factors for C and R, respectively
e^A and e^{MM}	=	Errors in fracture toughness assessment corresponding to the traditional (averaging) method and the method with mode-mixity, respectively
G	=	Strain energy release rate
G_c	=	Interfacial fracture toughness of the sandwich structure
K_I and K_{II}	=	Mode I and mode II stress intensity factors, respectively
P_{design}, W_{design} and t_{design}	=	Design load, weight and thickness of the structure, respectively
S_F	=	Safety factor of 1.5
VAR_C and VAR_R	=	Variabilities of C and R, respectively
w and σ_a	=	Width and allowable stress for the representative structure
ψ	=	Mode-mixity angle

I. Introduction

STRUCTURAL design of aerospace structures is still performed with deterministic design philosophy. Researchers are constantly improving the accuracy of structural analysis and failure prediction. This improvement in accuracy reduces uncertainty in aircraft design and can therefore be used to enhance safety. However, since the record

[*] Research Assistant, Dept. of Mechanical and Aerospace Engineering, AIAA Student Member. eacar@ufl.edu
[†] Distinguished Professor, Dept. of Mechanical and Aerospace Engineering, AIAA Fellow. haftka@ufl.edu
[‡] Ebaugh Professor, Dept. of Mechanical and Aerospace Engineering, AIAA Associate Fellow. sankar@ufl.edu
[§] Senior Engineer, Structural Mechanics Department. qiuxueshi@yahoo.com.cn

of structural safety in civilian transport aircraft is very good, it makes sense to ask how much the design load can be increased or the weight can be reduced if safety is to be maintained at a specified level. Currently, there is no accepted way to translate the improvement in accuracy to weight savings or increased design loads. The objective of this paper is to take a first step in this direction by utilizing probabilistic design methodology. Haftka (2005) describes how Starnes' work (e.g., Li et al.,1997, Arbocz and Starnes, 2002) to reduce variability in predicting buckling of circular cylinder inspired work in his research group on the effect of variability control on reducing the weight of composite liquid hydrogen tanks. Qu et al. (2003) showed that for fixed probability of failure small reductions in variability can be translated to substantial weight savings. Here we seek to investigate the potential of reduction in errors.

Sandwich structures are used in aerospace vehicles due to their low areal density and high stiffness. However, debonding of core from the face sheet is a common failure mode in sandwich construction, and the interfacial fracture is traditionally characterized by a single fracture toughness parameter. However, in reality the fracture toughness is a function of the relative amount of mode II to mode I (mode-mixity) acting on the interface (Suo, 1999). Stiffness of sandwich structures depends very much on the integrity of the face sheet/core bonding. Even a small disbond can significantly reduce the load carrying capacity, especially when the structure is under compressive loads (Avery and Sankar, 2000; Sankar and Narayanan, 2001). Grau et al. (2005) measured the interfacial fracture toughness as a function of mode-mixity to characterize the propagation of the disbond between the face sheet and the core. They performed asymmetric double cantilever beam fracture tests to determine the interfacial fracture toughness of the sandwich composite, and then demonstrated its application in predicting the performance of a sandwich structure containing a disbond. The use of mode-mixity dependent fracture toughness led to improvement in the accuracy of failure prediction of debonded structures. In this paper we perform probabilistic analysis of the debonded sandwich structure analyzed by deterministic approach by Grau et al. (2005) to explore a possible increase in the design load of the structure.

Next, with the question of trading weight for accuracy improvement in mind, we analyze structural failure of a representative aircraft structure due to point stress failure. Here we do not model damage propagation in the structure, for example, due to fatigue, corrosion, impact damage, etc. We make use of our previous work (Kale et al., 2004, Acar et al., 2004), which explored the effects of errors, variability and safety measures on the probability of failure of aircraft structural components. We utilize probabilistic design methodology to translate reductions in error bounds to weight reduction for fixed probability of structural failure.

The following section discusses the structural design of a sandwich structure and a representative aircraft structure. Section 3 presents the analysis of structural uncertainties with the main perspective of how to control uncertainty. Section 4 gives the general form of probability of failure in terms of loading, weight and uncertainty. Section 5 discusses the tradeoffs of accuracy against increasing design load or reducing weight of structures. Section 6 presents the quantification of errors and variability for the sandwich structure and the representative aircraft structure. Section 7 shows the results of increase in the design load of the sandwich structure and the weight savings from the representative aerospace structure by reducing errors. Finally, concluding remarks are given in the last section.

II. Structural Analyses of a Sandwich Structure and a Representative Aircraft Structure

In this section, we introduce the structural design analysis of the two structures that we analyzed in this paper. First, we introduce the structural design analysis of a sandwich structure, for which we explore the effects of error reduction on increasing the design load of the structure in the following sections. Next, we introduce a representative aircraft structure designed for point stress failure. For this representative structure we investigate the effects of error reduction on the weight savings from the structure in the following sections.

A. Structural Analysis of a Sandwich Structure

Sandwich panels are susceptible to debonding of the face sheet from the core. This is similar to the phenomenon of delamination in laminated composites. Disbonds could develop due to poor manufacturing or during service, e.g., foreign object impact damage. Evaluation of damage and prediction of residual strength and stiffness of debonded sandwich panels is critical because the disbonds can grow in an unstable manner and can lead to catastrophic failure. Stiffness of sandwich structures depends very much on the integrity of the face sheet/core bonding. Even a small disbond can significantly reduce the load carrying capacity, especially when the structure is under compressive loads (Avery and Sankar, 2000; Sankar and Narayanan, 2001). Under compressive loads the debonded face sheet can buckle and create conditions at the crack tip that are conducive for unstable propagation of the disbond.

Fracture at the interface between dissimilar materials is a critical phenomenon in many multi-material systems including sandwich construction. Traditionally, in engineering practice, the interfacial fracture was characterized by

a single fracture toughness parameter obtained by averaging the interfacial fracture toughness, hereinafter termed as "average G_c" or $\overline{G}_c$, obtained for some number of K_I and K_{II} combinations, where K_I and K_{II} are the mode I and mode II stress intensity factors, respectively. Later, studies have indicated, e.g., Suo (1990), that for these multi-material systems, the interfacial fracture is a strong function of the relative amount of mode II to mode I acting on the interface, hereinafter termed as "G_c with mode-mixity" or simply G_c. The criterion for initiation of crack advance in the interface can be stated as

$$G_c = G_c(\psi), \qquad \psi = \tan^{-1}(K_{II} / K_I) \tag{2.1}$$

where G is the strain energy release rate and G_c is the interfacial fracture toughness that depends on the mode-mixity angle ψ. In bimaterial fracture, K_I and K_{II} are the real and imaginary parts of the complex stress intensity factor K. The toughness of interface $G_c(\psi)$ can be thought of as an effective surface energy that depends on the mode of loading.

Grau et al. (2005) analyzed a debonded sandwich panel, and determined the maximum internal gas pressure in the core before the disbond could propagate. They used interfacial fracture mechanics concepts to analyze this problem. The main premise here is that the crack will propagate when the energy release rate equals the fracture toughness for the core/face-sheet interface. This problem has become very significant after the historic failure of X-33 vehicle fuel tank made of a sandwich design of PMC face sheets and honeycomb core. The load and boundary conditions for the model problem are depicted in Figure 1.

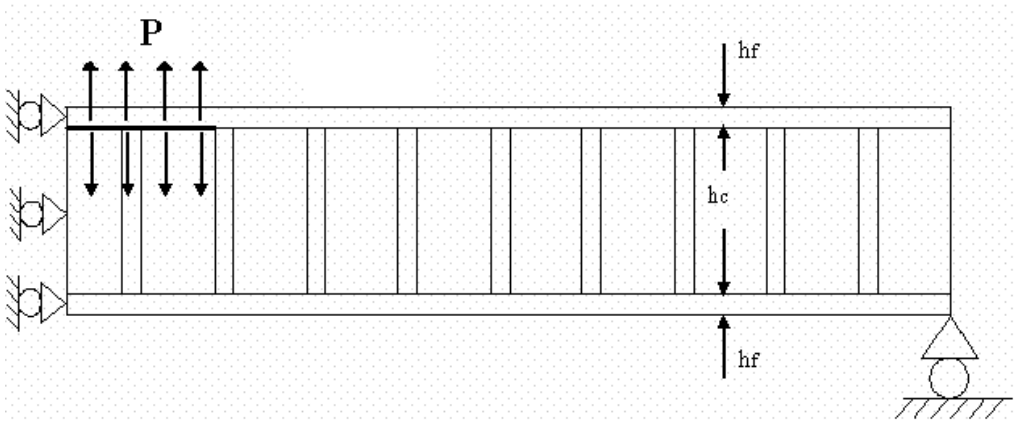

Figure 1. The model of face-sheet/core debonding in a one-dimensional sandwich panel with pressure load. *Note that half of the structure is modeled.*

The maximum allowable pressure for a given disbond length is calculated from the energy release rate for a unit applied pressure p. The energy release rate G is proportional to the square of the applied load or

$$G = G_0 p^2 \tag{2.2}$$

where G_0 is the energy release rate due to unit pressure for a given sandwich panel and disbond configuration and p is the applied pressure. The critical pressure $p_{\max}$ can be obtained using

$$p_{\max} = \sqrt{\frac{G_c}{G_0}} \tag{2.3}$$

where G_c is the interfacial fracture toughness of the sandwich material system obtained from testing and G_0 is the energy release rate corresponding to the unit pressure obtained from Eq. (2.3).

Grau (2003) conducted asymmetric Double Cantilever Beam (DCB) tests to determine the interfacial fracture toughness of the sandwich composite (The face sheet material was A50TF266 S6 Class E, Fiber designation T800HB-12K-40B, matrix 3631 and the core sheet material was Euro-Composites aramid (ECA) fiber type honeycomb.). Grau et al. (2005) performed finite element analyses to compute the mode-mixity angle corresponding to

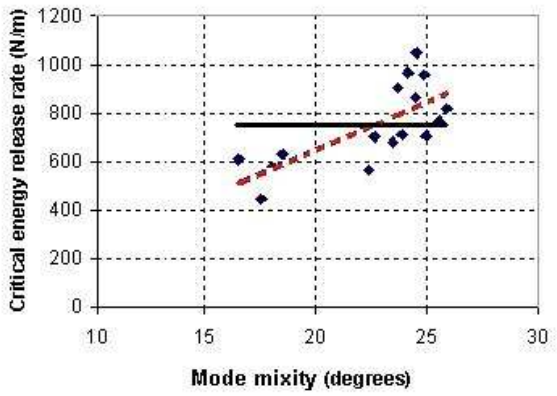

Figure 2. Critical energy release rate as a function of mode mixity. *Continuous line denotes average G_c ($\overline{G}_c$) and the dashed line denotes a linear least square to fit to G_c as a function of mode-mixity angle.*

designs tested in experiments. The average interfacial fracture toughness prediction and the fracture toughness in terms of mode-mixity angle are presented in Fig. 2.

As shown in Fig.2, a simple way of determining the interfacial fracture toughness parameter is to perform tests over a range of mode-mixity values and to take the average. However, as seen from Fig. 2 that the critical energy release rate is assessed better as a function of mode-mixity. Grau et al. (2005) represent the critical energy release rate as a linear function of the mode-mixity that improves the accuracy of estimate of G_c. In the following sections, we explore the effect of improvement in accuracy of G_c estimation on the design load of a sandwich structure.

B. Structural Analysis of a Representative Aircraft Structure

As noted earlier, aircraft structural design is still done by using code-based design rather than probabilistic approaches. Safety is improved through conservative design practices that include use of safety factors and conservative material properties. FAA regulation FAR-25.303 states that aircraft structures need to be designed with a safety factor to withstand 1.5 times the limit-load without failure. For use of conservative material properties, FAR-25.618 states that A-basis[**] or B-basis[**] material properties should be used in the design. If there is redundancy, B-basis value is used, otherwise A-basis value is used. In this work, we do not include redundancy in the analysis. The A-basis property is determined by calculating the value of a material property exceeded by 99% of the population with 95% confidence. Besides safety factor and conservative material properties, the safety of structures is also improved by tests of components and certification tests that can reveal inadequacies in analysis or construction. Certification tests improve the safety mainly by updating the distribution of errors in a conservative way. The effect of certification tests on the probability of failure of aircraft structures and the details of probability of failure calculations can be found in our previous papers (Kale et. al. 2004, Acar et al, 2004).

We consider a representative element (with representative length w and thickness t) in an aircraft structural component such as an element of wing skin, fuselage or engine blades such that the design variable for the element is the thickness. For this element, the stress is calculated from

$$\sigma = \frac{P}{wt} \tag{2.4}$$

where P is the applied on the small element. The design thickness is determined so that the calculated stress in the element is equal to material allowable stress for a design load P_d multiplied by a safety factor S_F, hence the design thickness of the representative element is calculated from Eq. (2.4) as

$$t_{design} = \frac{S_F P_d}{w\sigma_a} \tag{2.5}$$

σ_a is the allowable stress, i.e., A-basis value for the failure stress.

After the element has been designed by Eq. (2.5), we assume that for certification the element is loaded with the design axial force of (S_F times P_d). If this stress exceeds the failure stress then the design is rejected, otherwise it is certified for use. That is, the element is certified if the following inequality is satisfied

[**] A-basis value is the value exceeded by the 99% of the population with 95% confidence. B-basis value is the value exceeded by 90% of the population with 95% confidence. If there is redundancy, B-basis value is used, otherwise A-basis value is used.

$$\sigma - \sigma_f = \frac{S_F P_d}{wt} \le 0 \tag{2.6}$$

III. Analysis of Structural Uncertainties

A good review of different sources of uncertainty in engineering modeling and simulations is provided by Oberkampf et al. (1999, 2000). We simplify the classification as shown in Table 1 to distinguish between uncertainties that apply equally to the entire fleet of a structural component and uncertainties that vary for an individual structure. In addition, this simple classification makes it easy to analyze the effects uncertainty control. The uncertainties that affect the entire fleet are called here errors. They reflect inaccurate modeling of physical phenomena, errors in structural analysis, errors in load calculations, or use of materials and tooling in construction that are different from those specified by the designer. The aleatory uncertainty reflects variability in material properties, geometry, or loading between different copies of the same structure.

Table 1. Uncertainty Classification

Type	Spread	Cause	Remedies
Error (mostly epistemic)	Departure of the average fleet of an aerospace structure model (e.g. Boeing 737-400 from an ideal)	Errors in predicting structural failure, construction errors, deliberate changes	Testing and simulation to improve math model and the solution.
Variability (aleatory)	Departure of an individual structure from fleet level average	Variability in tooling, manufacturing process, and flying environment	Improve tooling and construction. Quality control.

IV. Assessment of Probability of Failure

Probability of failure of a structural component can be expressed in terms of its structural response R (e.g., stress) and its capacity C corresponding to that response (e.g., failure stress) by

$$P_f = \Pr(C \le R) \tag{4.1}$$

The structural response R is usually a function of several parameters such as the applied load P and the geometric parameters (and hence weight W). The capacity C is generally a material property, for instance failure strength. Both the response R and the capacity C have variability that needs to be included in the calculation of the probability of failure. Therefore, the response R and the capacity C can be represented in compact form as

$$R = R\,(VAR_R, P, W), \qquad C = C\,(C_0, VAR_C) \tag{4.2}$$

where C_0 is the nominal value of the capacity C, VAR_R and VAR_C represent the variability (i.e. randomness) in structural response and capacity, respectively. Due to errors in assessing R and C (e.g., errors in load, stress and material property calculations), the calculated values of R and C are different from their actual values. The calculated values of the response R and capacity C can be expressed in terms of the actual values by introducing error parameters e_R and e_C

$$R_{calc} = (1 + e_R) R_{act}, \qquad C_{calc} = (1 - e_C) C_{act} \tag{4.3}$$

The error parameter e_R stands for all errors related to the calculation of structural response such as errors in stress calculation, load calculation and geometry parameters. For the details of combining different sources of errors into a single error parameter, the reader is referred to Acar et al (2004). Similarly, e_C represents the error in predicting the capacity of the structure. Note that Eqs. (4.3) are formulated in such a way that a positive error leads to a conservative design.

The general equation for probability of failure given in Eq. (4.1) can be expressed as

$$P_f = \text{Prob}\left(\frac{1}{1-e_C} C_{calc}\left(C_0, VAR_C\right) - \frac{1}{1+e_R} R_{calc}\left(VAR_R, P, W\right) \le 0 \right) \tag{4.4}$$

Then, the probability of failure can be written in compact form as

$$P_f = P_f\left(e_C, C_0, VAR_C, e_R, VAR_R, P, W\right) \tag{4.5}$$

V. Tradeoffs of accuracy and design load and weight

We propose in this paper that the improvements in accuracy can be traded for increasing the design load of the structure or alternatively the weight of the structure can be reduced as discussed in the following two sub-sections.

A. Tradeoff of accuracy and design load

As seen from Eq. (4.5) that the probability of failure depends on the nominal value of capacity C_0, error parameters e_R and e_C, the variabilities VAR_C *and* VAR_R, the weight W and the applied load P. This indicates four distinct ways to increase the design load of a structure

(a) Use different material to increase C_0.
(b) Develop new techniques yielding more accurate solutions that reduce the error parameters e_R and e_C.
(c) Improve quality control and manufacturing processes to reduce variability between nominally identical structural components.
(d) Use a higher safety factor (S_F) leading to more conservative and heavier design.

We see from Eq. (4.5) that it is possible to use (b) or (c) to increase the design load of the structure while still keeping the weight unchanged. The FAA specifies the use of A-basis or B-basis properties that add a safety factor on material allowables that depends on variability. For example, a standard deviation of 10% in failure stress translates to more than 20% reduction in the allowable design stress using A-basis properties. Similarly, Qu et al. (2001) found that the application of quality controls to detect and reject material with low failure stress reduces the probability of failure significantly. Here we propose that we can similarly increase the design load of structures by improving accuracy.

For a target probability of failure $\left(P_f\right)_{\text{target}}$, the design load can be calculated from

$$\text{Prob}\left(\frac{1}{1-e_C} C_{calc}\left(C_0, VAR_C\right) - \frac{1}{1+e_R} R_{calc}\left(P_{design}, W, VAR_R\right) \le 0 \right) = \left(P_f\right)_{\text{target}} \tag{5.1}$$

We will illustrate this with sandwich structure design problem, for which the structural response is $R=G_0 p^2$, and the capacity is $C=G_c$. Here, we consider only the error in the capacity G_c of the structure. In addition, the variability in both the structural capacity and response is taken into account. We consider the use of a more accurate model (the method that uses mode-mixity) for the interfacial fracture toughness prediction of sandwich structures that will reduce e_C. Thus, given the target probability of failure, the design loads corresponding to different error factors can be calculated from Eq. (5.2).

$$P_f\left(e_{C_1}, P_{design_1}\right) = P_f\left(e_{C_2}, P_{design_2}\right) = \left(P_f\right)_{\text{target}} \tag{5.2}$$

The design load P_{design} of the sandwich structure can be also assessed using deterministic design philosophy. In that case, the safety factor of 1.4 (commonly used for space applications) for loads and conservative material properties (B-basis values) are used. For the sandwich structure, we approximate the probability of failure by considering the system failure of two parallel connected structures to simulate redundancy with normally distributed limit-state functions. The sandwich panels do not have normally distributed limit-state function, so that the use of Eq (5.3) provides only an approximation.

$$\beta_S = \beta_C \sqrt{\frac{n}{1+\rho(n-1)}} \tag{5.3}$$

In Eq. (5.3), β_S is the reliability index for the system made of n components, β_C is the reliability index for the components (here n=2) and ρ is the correlation coefficients (here it is assumed to be 0.5) of the limit states of the components. The details of calculation of component probability of failure by analytical means are given in Appendix I. Recall that the relationship between the reliability index β and the probability of failure is given as

$$P_f = \Phi(-\beta) \tag{5.4}$$

where Φ is the cumulative distribution function f the standard normal distribution.

B. Tradeoff of accuracy and weight

Alternatively, for a given probability of failure, it is possible to reduce the safety factor, i.e., reduce the weight by either reducing the error or reducing the variability. We propose that we can trade changes in the safety factor (hence the weight) against changes in accuracy, while still maintaining the same probability of failure level. The changes in the safety factors may require changes to FAA mandated safety factors that will allow flexible safety factors based on accuracy, or they may require changes in company practices that enforce additional conservative design practices above the formal requirements.

The calculation of weight savings is similar to the calculation of the increase in design load. For weight savings, we consider the design of a representative aircraft structure that we discussed earlier. For this problem, the structural response is $R=P/wt$ and the capacity is $C=\sigma_f$. In the composite structure example, we consider the error in the capacity of the structure, e_C. However, for this problem we consider the error in the structural response, e_R. The variability in both the structural capacity and response are also taken into account. We calculate the weight savings from the structure corresponding to different error factors from Eq. (5.5). The details of calculation of probability of failure for this problem are given in Appendix II.

$$P_f\left(e_{R_1}, W_1\right) = P_f\left(e_{R_2}, W_2\right) = \left(P_f\right)_{\text{target}} \tag{5.5}$$

VI. Analysis of Error and Variability

A. Quantification of Variability and Errors for the Sandwich Structure

As noted earlier, one way of controlling errors is improving the accuracy of analysis by using more sophisticated analysis techniques. Grau et al. (2005) consider the problem of a pressure vessel similar to the liquid hydrogen tank of the X-33 reusable flight demonstration vehicle to demonstrate the usefulness of fracture mechanics approach for debonded sandwich structures. They explored the effect of mode mixity on the interfacial fracture toughness of sandwich composites, and study the effects on the residual strength of a debonded structure. In the present work we analyze the same problem by probabilistic approach and investigate the effect of improved accuracy associated with using mode-mixity on the design load.

1. Variability

We consider that the mode-mixity dependent G_c accurately represents the physical phenomenon. However, we notice in Fig. 2 that the G_c values obtained from experiments (performed by Grau et al., 2005) are different than mode-mixity dependent G_c. We assume that this deviation represents the variability. It is given in the third column of Table 2. Each row of Table 2 corresponds to a different design having a different mode-mixity angle, which is calculated through finite element analysis. Approximate probability density function for this variability is obtained by using ARENA software, which is a product of Systems Modeling company. The distribution parameters and goodness of fit statistic are given in Fig. 3. The corresponding p-value given in Fig. 3 is a measure for goodness of the fit. The p-values fall between 0 and 1 and larger p-values indicate better fits (Kelton et al., 1998). The p-values less than about 0.05 indicate that the distribution is not a good fit. In our case, the p-values are larger than 0.15, so we have good fits for probability density functions.

In addition to variability in G_c predictions, there is also variability in P. We assume that the maximum lifetime loading P follows lognormal distribution with mean value of P_{design} and coefficient of variation (*c.o.v.*) of 10%.

2. Errors

The fourth column of Table 2 presents the deviations of G_c values obtained through experiments from their average values. These deviations combine variability and error. Errors are due to neglecting the effect of mode-mixity in

G_c. Here, we do not perform a separate quantification for error and variability. Instead, we concentrate on total uncertainty. The distribution of uncertainty for this case is given in Figure 4.

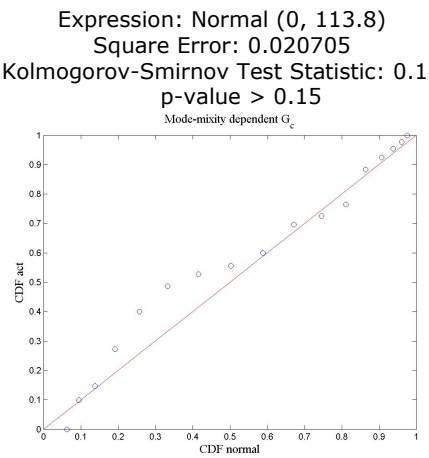

Figure 3. Comparison of actual and fitted cumulative distribution functions of variability of G_c (fitting is performed by using ARENA).

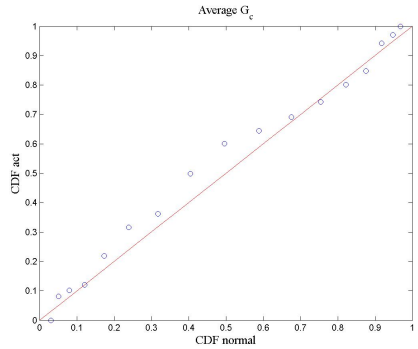

Figure 4. Comparison of actual and fitted cumulative distribution functions of total uncertainty (error and variability) of G_c (fitting is performed by using ARENA).

Table 2. Quantification of Uncertainty in the "average G_c" and "G_c with mode mixity" for different designs. *The superscript 'A' denotes the use of average fracture toughness and 'MM' indicates the use of mode-mixity dependent fracture toughness and 'u' represents the uncertainty.*

Design	ψ (deg)	% u^A	% u^{MM}
1	16.52	-137.1	-3.7
2	17.53	-303.5	6.3
3	18.05	-168.7	1.2
4	18.50	-117.9	13.1
5	22.39	-180.9	-14.9
6	23.89	-35.6	13.3
7	24.50	116.8	-5.5
8	24.89	209.6	-22.5
9	23.48	-67.1	8.8
10	24.98	-39.1	-0.7
11	25.55	20.5	-10.3
12	25.90	71.3	-25.1
13	22.65	-44.3	-11.0
14	23.69	157.1	2.5
15	24.15	218.4	-18.3
16	24.54	300.7	-16.6
	Std. Dev.	**162.2**	**113.8**

* Table 3 of Grau et al. (2005) is used to calculate the errors

Comparing the standard deviation of *error & variability* (u^A) to that *variability* only (u^{MM}) given in the last row of Table 2, we see that the improvements in the accuracy of G_c prediction (that is, reducing errors) leads to reduction of the total uncertainty by 30%. In the next section, we analyze the effect of this reduction on the design load.

B. Quantification of Errors and Variability for Representative Structural Element

1. Variability

Here we have variability in loading, material properties and geometric parameters. As we noted earlier, variability reflects departure the properties between different copies of the same structure. A summary of the distributions for these random variables listed in Table 3, which is taken from Kale et al. (2004).

2. Errors

For the representative structural element, we condense errors in load calculation, stress calculation, material properties and geometry parameters into a representative single error parameter e_R. So, the calculated stress is expressed as

$$\sigma_{calc} = (1 + e_R)\sigma_{true} = (1 + e_R)\frac{P}{wt} \tag{6.1}$$

where P is the applied load on the small element. Because of the error e_R, the design thickness formulated in Eq. (2.5) is replaced by

$$t_{design} = (1 + e_R)\frac{S_F P_d}{w\sigma_a} \tag{6.2}$$

Certification testing described earlier updates the probability distribution of error, which is initially assumed to be uniform distribution. The simplicity of the error distribution helps us o perform a detailed analysis by utilizing the derivatives of probability of failure with respect to error bound, safety factor and the design thickness as illustrated in Appendix III.

Table 3. Variability and Error for the representative aircraft structure

Variables	Distribution	Mean	Scatter
Length (w)	Uniform	1.0	(1%) bounds
Thickness (t)	Uniform	t_{design}	(3%) bounds
Failure stress (σ_f)	Lognormal	150.0	10 % c.o.v.
Service Load (P)	Lognormal	100.0	10 % c.o.v.
Error factor (e_R)	Uniform	0.0	0% to 50%

VII. Results

The percent increase in design load of the sandwich structure and weight savings from the representative aircraft structure as a result of error reduction are presented in the following sub-sections.

A. Increase in Design Load of the Sandwich Structure

We first compute the design load P_{design} by deterministic design philosophy. As noted earlier, the safety factor of 1.4 for loads and conservative material properties (B-basis values) are used. For the sandwich structure, we calculate the probability of failure by considering the system failure of two parallel connected structures. Since we impose redundancy, B-basis value for G_c, is used. The correlation coefficient between the two components is taken as 0.5. The design load and the probability of failure values are presented in Table 4.

Table 4. Design load and corresponding probabilities of failure of the sandwich panels designed via deterministic approach. *The superscript 'A' denotes the use of average fracture toughness of experiments and 'MM' indicates the use of mode-mixity dependent fracture toughness.*

Design	Design Load			Probability of Failure	
	$(P_{design})^A$ (kPa)	$(P_{design})^{MM}$ (kPa)	% Δp	$(P_f)^A$ (10^{-4})	$(P_f)^{MM}$ (10^{-4})
1	65.6	58.0	-11.7	54.73	26.18
2	342.2	311.4	-9.0	54.74	16.72
3	203.3	195.3	-3.9	54.74	6.88
4	98.8	100.5	1.7	54.74	2.47
5	58.0	60.7	4.8	54.74	1.43
6	316.8	298.8	-5.7	54.74	9.38
7	197.5	196.3	-0.6	54.74	3.79
8	93.7	98.2	4.8	54.73	1.43
9	54.8	59.0	7.6	54.74	0.86

10	316.8	298.5	-5.8	54.74	9.56
11	187.4	184.7	-1.5	54.73	4.42
12	89.9	92.6	3.0	54.74	1.97
13	52.3	55.1	5.3	54.74	1.30
	Average		**-0.8**	**54.74**	**6.65**

The second and third columns of the Table 4 show the design loads of the panels designed by using average G_c and by using G_c with mode-mixity, respectively. The fourth column shows the percent change of the design load if the use of G_c with mode-mixity is preferred over the use of average G_c. We see that the average over 13 designs is only -0.8%. That is the design load of the structure remains nearly the same. However, when we compare the probabilities of failure of the structures, we see that the average probability of failure reduced by more than a factor of eight.

Because the deterministic design is performed with fixed safety factors, improvements in accuracy reduce the probability of failure. Probabilistic analysis permits increasing instead the design load. Table 5 shows the comparison of design load for the average G_c and mode-mixity dependent G_c approaches.

Table 5. Design loads of the sandwich panels calculated via probabilistic approach. *The superscript 'A' denotes the use of average fracture toughness of experiments and 'MM' indicates the use of mode-mixity dependent fracture toughness.*

Design	$P_f = 5.47\times10^{-3}$		
	$(P_{design})^{A}$ (kPa)	$(P_{design})^{MM}$ (kPa)	% Δp
1	65.7	61.1	-7.0
2	342.0	335.7	-1.9
3	203.3	217.9	7.2
4	98.7	115.3	16.8
5	58.0	70.6	21.7
6	316.7	329.8	4.2
7	197.6	223.0	12.8
8	93.7	114.0	21.6
9	54.8	69.1	26.1
10	316.7	329.4	4.0
11	187.4	208.9	11.5
12	89.8	106.7	18.8
13	52.3	64.1	22.6
	Average		**12.2**

We see in Table 5 that the design load for the sandwich panels designed using 'G_c with mode-mixity' are larger on average than loads obtained by using 'average G_c' by about 12%.

B. Weight Savings from the Representative Element

Similar to the sandwich structure problem, we use probabilistic design methodology to calculate weight savings from the representative aircraft structure. The saving from the weight (i.e. the thickness) is calculated from Eq. (5.4) and plotted with respect to error bound is plotted in Figure 5. It is seen that reducing the error bound from 50% to 10%, provides about 24% savings in weight.

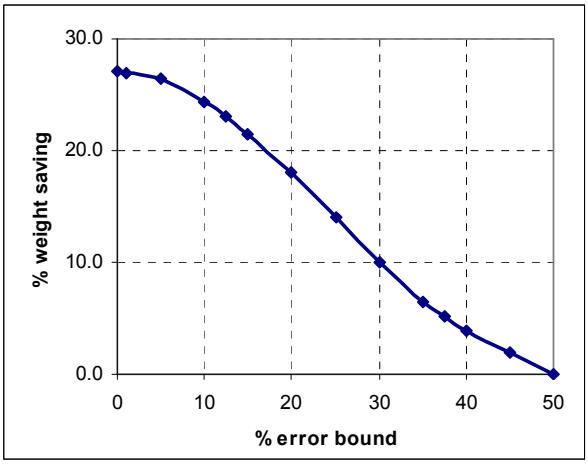

Figure 5. Weight savings from the representative element by error reduction

VIII. Concluding Remarks

The effect of error control on tradeoffs of design load, weight and safety of structures are analyzed by using probabilistic design methodology. We first analyzed the effect of error control on design load of structural components. The example is a sandwich structure analyzed by Grau et al. (2005). The error control mechanism here is the use of a more sophisticated failure (the use of mode-mixity dependent fracture toughness) over the simpler failure

model (average fracture toughness). It is found that the design load of the structure can be increased by 12% by using G_c with mode-mixity instead of average G_c.

Next, we consider structural failure due to point stress without damage propagation, and illustrate by using a representative aircraft structure that improving the accuracy of structural analysis can allow weight reduction. The effects of the use of safety factor, conservative material properties and certification testing are taken into account in the analysis. The sensitivities of probability of failure and design thickness with respect to safety factor and error bound are calculated. It is found that reducing errors from 50% to 10% provides up to 24% savings in weight of the representative structure.

Appendix I

Calculation of F_G and P_f for the sandwich structure

The distribution of a function Z of two random variables X and Y, Z=h(X, Y) can be calculated as (Ang and Tang, 1975, p.170)

$$f_Z(z) = \int_{-\infty}^{\infty} f_{X,Y}(x,y)\left|\frac{\partial x}{\partial z}\right| dy \tag{A1.1}$$

where $f_{X,Y}(x,y)$ is joint probability distribution function of $x = h^{-1}(z,y)$ and Y and.

We can write the limit-state function for the sandwich panel problem as

$$g = (G_c)_{calc} - G_0 p^2 \tag{A1.2}$$

We calculate probability density function (PDF) of the limit state function g from PDF's of $(G_c)_{calc}$. Therefore, in Eq. (A1.1) we replace Z with g, X with $(G_c)_{calc}$, Y with p, and also we have $(G_c)_{calc} = g + G_0 p^2$. After performing these changes, we get from Eq. (A1.1) that

$$f_G(g) = \int_0^{\infty} f_{G_c,p}\left(g + G_0 p^2, p\right) dp \tag{A1.3}$$

Here we assume that G_C and p are statistically independent, hence the joint distribution in Eq.(A1.3) is calculated as

$$f_{G_c,p}(G_c, p) = f_{G_c}\left(g + G_0 p^2\right) f_p(p) \tag{A1.4}$$

and also we have $\left|\frac{\partial x}{\partial z}\right| = \left|\frac{\partial G_c}{\partial g}\right| = 1$

Then, the cumulative distribution function (CDF) of g is calculated as

$$F_G(g) = \int_{-\infty}^{g} f_G(g)\ dg \tag{A1.5}$$

which yields us to compute the probability of failure simply as $P_f = F_G(0)$.

Appendix II

Probability of failure calculation for the representative element

Failure is predicted to occur when the structural response R is greater than carrying capacity of the structure C. Then, the probability of failure is given as

$$P_f = \Pr(C \le R) \tag{A2.1}$$

where

$$R = \frac{P}{w\,t(e)} \text{ and } C = \sigma_f \tag{A2.2}$$

Since the coefficient of variations of t and w is small compared to the coefficient of variation of P(see Table 3 in the main text), R can be approximated as lognormal to take advantage of the properties of lognormal distribution for calculating the distribution parameters. Hence, both C and R are lognormally distributed random variables with distribution parameters λ_C, ζ_C, λ_R and ζ_R. Then, from Eqs. (A2.2) the distribution parameters can be obtained as

$$\lambda_R(e) = \lambda_P - \lambda_t(e) - \lambda_w \text{ and } \zeta_R^2 = \zeta_P^2 + \zeta_t^2 + \zeta_w^2 \tag{A2.3}$$

where

$$\lambda_t(e) = \ln(t_{design}(e)) - 0.5\zeta_t^2 = \ln\left((1+e)\frac{S_F P_d}{w\sigma_a}\right) - 0.5\zeta_t^2 \tag{A2.4}$$

and λ_R and ζ_R are the distribution parameters of the failure stress.

Then, P_f can be calculated as

$$P_f = P(C \le R) = \Phi\left(\frac{\lambda_R(e) - \lambda_C}{\sqrt{\zeta_R^2 + \zeta_C^2}}\right) = \Phi\big(-\beta(e)\big) = \int_{-\infty}^{-\beta(e)} \frac{1}{\sqrt{2\pi}} \exp\left(-\frac{x^2}{2}\right) dx \tag{A2.5}$$

Appendix III

Sensitivity Analysis for Probability of Failure of the Representative Structural Element and Analytical Calculation of Partial Derivatives of Probability of Failure

For the case of a uniformly distributed errors between ($-b_e$, b_e) we can use the following simple derivation to obtain the effect of error reduction on the design thickness of the representative structural element for fixed probability of failure. To attain the probability of failure at a specified level, we equate the total derivative of probability of failure to zero. Recall that probability of failure is expressed in compact form as

$$P_f = P_f\big(e_C, C_0, VAR_C, e_R, VAR_R, P, W\big) \tag{4.5}$$

For the representative structure, we keep variables except e_R and W unchanged. The weight W is a function of safety factor S_F used in the design and the probability distribution of error e_R is only dependent on the error bound b_e. So, probability of failure is a function of error bound b_e and safety factor S_F. Thus, the total derivative of probability of failure can be expressed as we have

$$d\overline{P}_f = \frac{\partial \overline{P}_f}{\partial b_e} db_e + \frac{\partial \overline{P}_f}{\partial S_F} dS_F = 0 \tag{A3.1}$$

So, given the change in error bound and safety factor, the change in failure probability can be calculated. Similarly, the total derivative of design thickness is

$$dt_{design} = \frac{\partial t_{design}}{\partial b_e} db_e + \frac{\partial t_{design}}{\partial S_F} dS_F \tag{A3.2}$$

Imposing the condition that the failure probability to be attained at the same value (i.e. Eq. (A3.1)) we obtain the thickness change depending on the bound of error

$$dt_{design} = \left(\frac{\partial t_{design}}{\partial b_e} - \frac{\partial t_{design}}{\partial S_F} \frac{\partial \overline{P}_f / \partial b_e}{\partial \overline{P}_f / \partial S_F}\right) db_e \tag{A3.3}$$

which gives the saving from the structural weight of the aircraft component. Since we choose a representative component and a simple failure mode, the derivatives are calculated by analytical means, which is given in the next sub-

section of this appendix. For a more complex geometry and complex failure model, numerical differentiation can be employed.

We calculate the partial derivatives of probability of failure with respect to the error bound b_e and with respect to the safety factor. Hence, given the change in error bound and safety factor, the change in failure probability can be calculated. These derivatives are shown as function of the error bound in Figure A3.1.

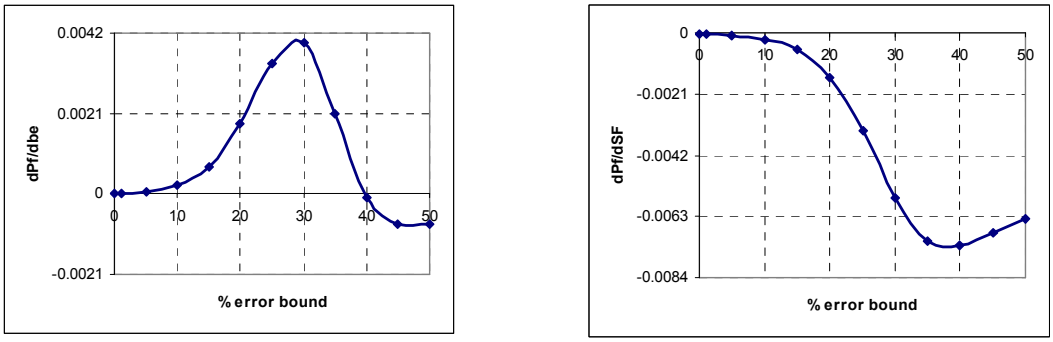

(a) **(b)**

Figure A3.1. Variation of Partial Derivatives of $\overline{P}_f$ with error bound b_e (for S_F =1.5)
(a) derivative with respect to error bound b_e (b) derivative with respect to S_F

Next, we calculate the partial derivatives of design thickness with respect to the error bound b_e and with respect to the safety factor. The derivatives as function of the error bound are presented in Figure A3.2.

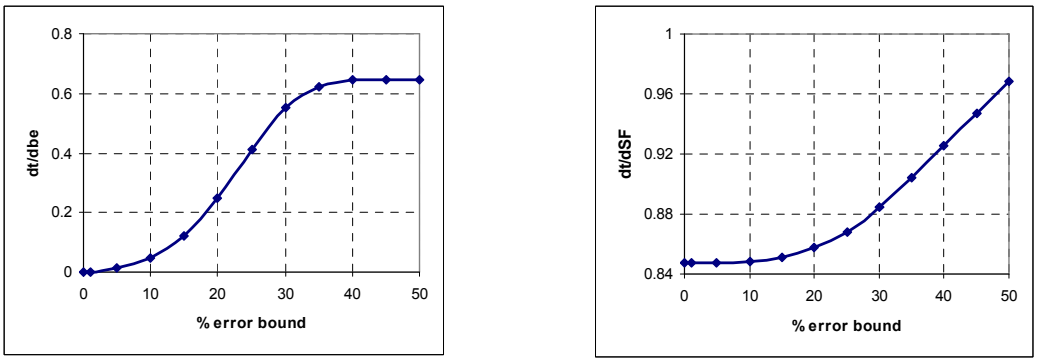

(a) **(b)**

Figure A3.2. Variation of Partial Derivatives of design thickness with error bound b_e
(a) derivative with respect to error bound b_e (b) derivative with respect to S_F

Finally, we use Eq. (A3.3) to calculate the total derivative dt_{design} by using the partial derivatives that we calculated before. The variation of this total derivative with error bound is shown in Fig. A3.3(a). Integration of this expression over bound of error gives the reduction of thickness by error reduction. The saving from the thickness (i.e. the weight) with respect to error bound is plotted in Fig. A3.3(b). It is seen that reducing the error bound from 50% to 10%, provides about 24% savings in weight.

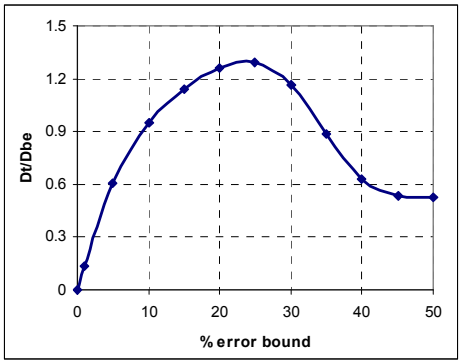

(a)

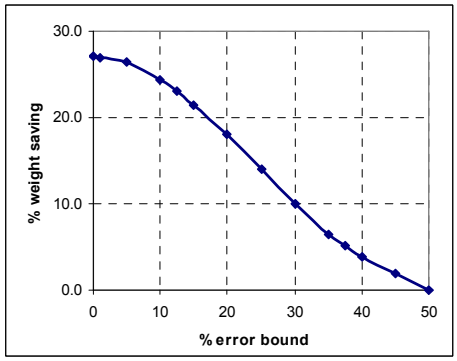

(b)

Figure A3.3. Effect of error bound on weight saving
(a) the effect on total derivative of thickness (b) the effect on the thickness

Analytical calculation of partial derivatives of probability of failure

For the representative structural element, the capacity of the structure is C=σ_f while the response of the structure is R=P/wt. Since we assume that w and t are also lognormally distributed, then R also has lognormal distribution. Since capacity C and resistance R both have lognormal distributions, then the probability of failure is easily calculated by analytical means as

$$P_f = \Phi\left(-\frac{\lambda_C - \lambda_R}{\sqrt{\zeta_C^2 + \zeta_R^2}}\right) \tag{A3.4}$$

where

$$\lambda_R = \lambda_P - \lambda_w - \lambda_t \tag{A3.5}$$

and

$$\zeta_R^2 = \zeta_P^2 + \zeta_w^2 + \zeta_t^2 \tag{A3.6}$$

The terms involved in Eqs. (A3.5) and (A3.6) are all constant except λ_t. Given the mean and standard deviation of the distributions, these distribution parameters are calculated from

$$\zeta = \sqrt{\ln\left(1 + \frac{\sigma^2}{\mu^2}\right)} = \sqrt{\ln\left(1 + \delta^2\right)} \tag{A3.7}$$

where δ is the coefficient of variation and

$$\lambda = \ln(\mu) - \frac{1}{2}\zeta^2 \tag{A3.8}$$

However, since design thickness t_{design} is a function of error e_R, t_{design} is itself a random variable. Since we do not take the error in capacity e_C into account, we represent e_R simply as e. Recall from Eq. (6.2) that t_{design} is defined as

$$t_{design} = (1 + e)\frac{S_F P_d}{w\sigma_a} \tag{A3.9}$$

Therefore, the term λ_t is not constant but a function of t_{design} as given below.

$$\lambda = \ln\left(t_{design}\right) - \frac{1}{2}\zeta_t^2 \tag{A3.10}$$

The probability of failure can be re-written as

$$P_f = \Phi\{-[a\ln(t_{design})+b]\} \tag{A3.11}$$

where a and b are positive constants defined in terms of distribution parameters of w, t, σ_f and P given by

$$a = \frac{1}{\sqrt{\zeta_{\sigma_f}^2+\zeta_w^2+\zeta_t^2+\zeta_P^2}} = \frac{1}{\sqrt{\ln(1+\delta_{\sigma_f}^2)+\ln(1+\delta_w^2)+\ln(1+\delta_t^2)+\ln(1+\delta_P^2)}} \tag{A3.12}$$

$$b = a\left[\lambda_{\sigma_f}+\lambda_w-\frac{1}{2}\zeta_t^2-\lambda_P\right] = a\left[\ln(\mu_{\sigma_f})-\frac{1}{2}\ln(1+\delta_{\sigma_f}^2)+\ln(\mu_w)-\frac{1}{2}\ln(1+\delta_w^2)-\frac{1}{2}\ln(1+\delta_t^2)-\ln(\mu_P)+\frac{1}{2}\ln(1+\delta_P^2)\right] \tag{A3.13}$$

Inserting Eq. (A3.9) into (A3.11) yields

$$P_f = \Phi\left\{-\left[a\ln\left((1+e)\frac{S_F P_d}{w_d \sigma_a}\right)+b\right]\right\} \tag{A3.14}$$

Since error factor *e* is a random variable, probability of failure P_f is also random. An estimator for P_f is defined as

$$\overline{P}_f = \int_{e_{low}}^{e_{upp}} P_f f_e de \tag{A3.15}$$

where f_e is the probability density function of error factor *e*, e_{low} and e_{upp} are lower and upper bounds for *e*, respectively. To maintain the same $\overline{P}_f$ value, the total derivative of $\overline{P}_f$ should be zero.

$$d\overline{P}_f = \frac{\partial \overline{P}_f}{\partial e_{low}} de_{low} + \frac{\partial \overline{P}_f}{\partial e_{upp}} de_{upp} + \frac{\partial \overline{P}_f}{\partial a} da + \frac{\partial \overline{P}_f}{\partial b} db + \frac{\partial \overline{P}_f}{\partial S_F} dS_F \tag{A3.16}$$

and for finite changes Eq.(A3.13) can be written as

$$\Delta\overline{P}_f = \frac{\partial \overline{P}_f}{\partial e_{low}} \Delta e_{low} + \frac{\partial \overline{P}_f}{\partial e_{upp}} \Delta e_{upp} + \frac{\partial \overline{P}_f}{\partial a} \Delta a + \frac{\partial \overline{P}_f}{\partial b} \Delta b + \frac{\partial \overline{P}_f}{\partial S_F} \Delta S_F \tag{A3.17}$$

As a starting point, we assume $e_{upp} = -e_{low} = b_e$ and also assume no change in variability ($\Delta a = \Delta b = 0$) which yields

$$\Delta\overline{P}_f = \frac{\partial \overline{P}_f}{\partial b_e} \Delta b_e + \frac{\partial \overline{P}_f}{\partial S_F} \Delta S_F \tag{A3.18}$$

where

$$\overline{P}_f = \int_{-b_e}^{b_e} \Phi\left\{-\left[a\ln\left((1+e)\frac{S_F P_d}{w_d \sigma_a}\right)+b\right]\right\} f_e\, de = \int_{-b_e}^{b_e} \Phi\{h(e, S_F)\}\, f_e\, de \tag{A3.19}$$

and

$$h(e, S_F) = -\left[a\ln\left((1+e)\frac{S_F P_d}{w_d \sigma_a}\right)+b\right] \tag{A3.20}$$

$$\Phi(x) = \frac{1}{\sqrt{2\pi}} \int_{-\infty}^{x} \exp\left(-\frac{t^2}{2}\right) dt = \frac{1}{2}\left[1+erf\left(\frac{x}{\sqrt{2}}\right)\right] \tag{A3.21}$$

The updated distribution of error factor is obtained through Bayes' theorem as

$$f^U(e) = \frac{\Pr(\text{Passing Certification} \mid e)\, f^I(e)}{\int_{-b_e}^{b_e} P(C \mid e)\, f^I(e) de} \tag{A3.22}$$

where $f^I(e)$ is the initial distribution of the error factor e, and

$$\Pr(\text{Passing Certification} \mid e) = \Pr(C > R) = \Phi\left(\frac{\lambda_C(e) - \lambda_R}{\zeta_C^2 + \zeta_R^2}\right) = \Phi\left[h_c(e, S_F)\right] \tag{A3.23}$$

is the probability that the structure passes the certification testing. In Eq. (A3.23), the term h_c is similar to h defined earlier in (A3.20) and is expressed as

$$h_c(e, S_F) = \left[a_c \ \ln\left((1+e)\frac{S_F P_d}{w\sigma_a}\right) + b_c(S_F) \right] \tag{A3.24}$$

where the subscript 'c' stands for certification. Similarly, the terms a_c and b_c are expressed as

$$a_c = \frac{1}{\sqrt{\ln\left(1+\delta_{\sigma_f}^2\right) + \ln\left(1+\delta_w^2\right) + \ln\left(1+\delta_t^2\right)}} \tag{A3.25}$$

$$b_c(S_F) = a_c\left[\ln\left(\mu_{\sigma_f}\right) - \frac{1}{2}\ln\left(1+\delta_{\sigma_f}^2\right) + \ln\left(\mu_w\right) - \frac{1}{2}\ln\left(1+\delta_w^2\right) - \frac{1}{2}\ln\left(1+\delta_t^2\right) - \ln\left(S_F P_d\right) \right] \tag{A3.26}$$

Then, we can re-write the updated distribution of the error factor as

$$f^U(e, b_e, S_F) = \frac{\Phi\left[h_c(e, S_F)\right]\frac{1}{2b_e}}{\int_{-b_e}^{b_e} \Phi\left[h_c(e, S_F)\right]\frac{1}{2b_e} de} = \frac{\Phi\left[h_c(e, S_F)\right]}{\int_{-b_e}^{b_e} \Phi\left[h_c(e, S_F)\right] de} \tag{A3.27}$$

Thus we can write probability of failure as

$$\overline{P}_f = \int_{-b_e}^{b_e} \left(\Phi\left[h(e, S_F)\right] \frac{\Phi\left[h_c(e, S_F)\right]}{\int_{-b_e}^{b_e} \Phi\left[h_c(e, S_F)\right] de} \right) de = \int_{-b_e}^{b_e} \left(u(e, b_e, S_F)\right) de \tag{A3.28}$$

where

$$u(e, b_e, S_F) = \frac{1}{\int_{-b_e}^{b_e} \Phi\left[h_c(e, S_F)\right] de} \Phi\left[h(e, S_F)\right] \Phi\left[h_c(e, S_F)\right] \tag{A3.29}$$

Partial derivative with respect to error bound b_e

To calculate $\frac{\partial \overline{P}_f}{\partial b_e}$ we use Leibniz rule given in Eq. (A3.30)

$$\frac{\partial}{\partial z}\int_{a(z)}^{b(z)} f(x,z)dx = \int_{a(z)}^{b(z)} \frac{\partial f}{\partial z}dx + f\big(b(z),z\big)\frac{\partial b}{\partial z} - f\big(a(z),z\big)\frac{\partial a}{\partial z} \tag{A3.30}$$

Then, the partial derivative $\dfrac{\partial \overline{P}_f}{\partial b_e}$ is calculated from

$$\frac{\partial \overline{P}_f}{\partial b_e} = \int_{-b_e}^{b_e} \frac{\partial u}{\partial b_e}de + u\big(b_e, b_e, S_F\big) + u\big(-b_e, b_e, S_F\big) \tag{A3.31}$$

where

$$\frac{\partial u}{\partial b_e} = \Phi\big[h\big(e,S_F\big)\big]\Phi\big[h_c\big(e,S_F\big)\big]\frac{\partial}{\partial b_e}\left\{1/\int_{-b_e}^{b_e}\Phi\big[h_c\big(e,S_F\big)\big]de\right\} \tag{A3.32}$$

and the last term of Eq.(A3.32) can be re-written as

$$\frac{\partial}{\partial b_e}\left\{1/\int_{-b_e}^{b_e}\Phi\big[h_c\big(e,S_F\big)\big]de\right\} = \frac{-\dfrac{\partial}{\partial b_e}\left\{\displaystyle\int_{-b_e}^{b_e}\Phi\big[h_c\big(e,S_F\big)\big]de\right\}}{\left[\displaystyle\int_{-b_e}^{b_e}\Phi\big[h_c\big(e,S_F\big)\big]de\right]^2} \tag{A3.33}$$

where the numerator is evaluated by using the second fundamental theorem of calculus given in Eq. (A3.34)

$$\frac{d}{dx}\left[\int_a^x f(t)dt\right] = f(x) \tag{A3.34}$$

Hence, the numerator in Eq. (A3.33) reduces to

$$\frac{\partial}{\partial b_e}\left\{\int_{-b_e}^{b_e}\Phi\big[h_c\big(e,S_F\big)\big]de\right\} = \Phi\big[h_c\big(e,S_F\big)\big] + \Phi\big[h_c\big(-e,S_F\big)\big] \tag{A3.35}$$

Then, Eq. (A3.32) becomes

$$\frac{\partial u}{\partial b_e} = -\frac{\Phi\big[h_c\big(e,S_F\big)\big] + \Phi\big[h_c\big(-e,S_F\big)\big]}{\left[\displaystyle\int_{-b_e}^{b_e}\Phi\big[h_c\big(e,S_F\big)\big]de\right]^2}\Phi\big[h\big(e,S_F\big)\big]\Phi\big[h_c\big(e,S_F\big)\big] \tag{A3.36}$$

Finally, the desired partial derivative $\dfrac{\partial \overline{P}_f}{\partial b_e}$ is then obtained as

$$\frac{\partial \overline{P}_f}{\partial b_e} = -\frac{\Phi[h_c(e,S_F)]+\Phi[h_c(-e,S_F)]}{\left[\int_{-b_e}^{b_e}\Phi[h_c(e,S_F)]de\right]^2}\int_{-b_e}^{b_e}[\Phi[h(e,S_F)]\,\Phi[h_c(e,S_F)]]de$$
$$+\Phi[h(b_e,S_F)]\frac{\Phi[h_c(b_e,S_F)]}{\int_{-b_e}^{b_e}\Phi[h_c(e,S_F)]de}+\Phi[h(-b_e,S_F)]\frac{\Phi[h_c(-b_e,S_F)]}{\int_{-b_e}^{b_e}\Phi[h_c(e,S_F)]de} \quad \text{(A3.37)}$$

Partial derivative with respect to safety factor S_F

Partial derivative $\frac{\partial \overline{P}_f}{\partial S_F}$ for updated probability of failure is calculated as follows.

$$\frac{\partial \overline{P}_f}{\partial S_F} = \int_{-b_e}^{b_e}\frac{\partial u(e,b_e,S_F)}{\partial S_F}de \quad \text{(A3.38)}$$

where $u(e,b_e,S_F)$ is defined earlier in Eq. (A3.28). The derivative of u with respect to S_F can be written as

$$\frac{\partial u}{\partial S_F} = \frac{\partial}{\partial S_F}\left\{1/\int_{-b_e}^{b_e}\Phi[h_c(e,S_F)]de\right\}\Phi[h(e,S_F)]\Phi[h_c(e,S_F)]$$
$$+\left\{1/\int_{-b_e}^{b_e}\Phi[h_c(e,S_F)]de\right\}\left\{\frac{\partial\Phi[h(e,S_F)]}{\partial S_F}\Phi[h_c(e,S_F)]+\Phi[h(e,S_F)]\frac{\partial\Phi[h_c(e,S_F)]}{\partial S_F}\right\} \quad \text{(A3.39)}$$

The first partial derivative in Eq. (A3.39) is calculated as follows.

$$\frac{\partial\Phi\{h(e,S_F)\}}{\partial S_F} = \frac{1}{\sqrt{2\pi}}\frac{\partial}{\partial S_F}\left[\int_{-\infty}^{h(e,S_F)}\exp\left(-\frac{z^2}{2}\right)dz\right] \quad \text{(A3.40)}$$

Now, utilizing the chain rule and the second fundamental theorem of calculus given in Eq. (A3.34) we obtain

$$\frac{\partial\Phi[h(e,S_F)]}{\partial S_F} = \frac{1}{\sqrt{2\pi}}\left\{\frac{\partial}{\partial h}\left[\int_{-\infty}^{h(e,S_F)}\exp\left(-\frac{z^2}{2}\right)\right]dz\right\}\frac{\partial h}{\partial S_F} = \frac{1}{\sqrt{2\pi}}\left[\exp\left(-\frac{h^2(e,S_F)}{2}\right)\right]\frac{\partial h(e,S_F)}{\partial S_F} \quad \text{(A3.41)}$$

where

$$\frac{\partial h}{\partial S_F} = \frac{\partial}{\partial S_F}\left(-\left[a\ln\left((1+e)\frac{S_F P_d}{w_d\sigma_a}\right)+b\right]\right) = -\frac{a}{S_F} \quad \text{(A3.42)}$$

Then, Eq. (A3.40) reduces to

$$\frac{\partial\Phi[h(e,S_F)]}{\partial S_F} = -\frac{a}{\sqrt{2\pi}S_F}\left[\exp\left(-\frac{1}{2}h^2(e,S_F)\right)\right] \quad \text{(A3.43)}$$

The first partial derivative in Eq. (A3.39) is calculated as follows. The first term is easily obtained by noticing the similarity to Eq. (A3.42) as

$$\frac{\partial}{\partial S_F}\left(a_c \ln\left((1+e)\frac{S_F P_d}{w_d \sigma_a}\right)\right) = \frac{a_c}{S_F} \tag{A3.44}$$

and also Eq. (A3.26) reveals that

$$\frac{\partial}{\partial S_F}\left(b_c(S_F)\right) = -\frac{a_c}{S_F} \tag{A3.45}$$

Then, we have

$$\frac{\partial h_c}{\partial S_F} = \frac{\partial}{\partial S_F}\left(-\left[a_c \ln\left((1+e)\frac{S_F P_d}{w_d \sigma_a}\right) + b_c(S_F)\right]\right) = -\left(\frac{a_c}{S_F} - \frac{a_c}{S_F}\right) = 0 \tag{A3.46}$$

That leads to

$$\frac{\partial \Phi[h_c(e,S_F)]}{\partial S_F} = \frac{\partial}{\partial h_c}\left[\int_{-\infty}^{h_c} \frac{1}{\sqrt{2\pi}} \exp\left(-\frac{z^2}{2}\right) dz\right] \frac{\partial h_c}{\partial S_F} = 0 \tag{A3.47}$$

And thus we also get

$$\frac{\partial}{\partial S_F}\left\{1 \Big/ \int_{-b_e}^{b_e} \Phi[h_c(e,S_F)] de\right\} = -\frac{\int_{-b_e}^{b_e} \frac{\partial \Phi[h_c(e,S_F)]}{\partial S_F} de}{\left[\int_{-b_e}^{b_e} \Phi[h_c(e,S_F)] de\right]^2} = 0 \tag{A3.48}$$

Then, Eq. (A3.38) becomes

$$\frac{\partial u}{\partial S_F} = \left\{1 \Big/ \int_{-b_e}^{b_e} \Phi[h_c(e,S_F)] de\right\}\left\{-\frac{a}{\sqrt{2\pi} S_F}\left[\exp\left(-\frac{h^2(e,S_F)}{2}\right)\right]\right\} \Phi[h_c(e,S_F)] \tag{A3.49}$$

And finally we have

$$\frac{\partial \overline{P}_F}{\partial S_F} = \left\{1 \Big/ \int_{-b_e}^{b_e} \Phi[h_c(e,S_F)] de\right\} \int_{-b_e}^{b_e} \left\{-\frac{a}{\sqrt{2\pi} S_F}\left[\exp\left(-\frac{h^2(e,S_F)}{2}\right)\right]\right\} \Phi[h_c(e,S_F)] de \tag{A3.50}$$

Acknowledgments

This work has been supported by the NASA Constellation University Institute Program (CUIP), Ms. Claudia Meyer program monitor.

References

Acar, E., Kale, A. and Haftka, R.T. (2004). Effects of Error, Variability, Testing and Safety Factors on Aircraft Safety. *NSF workshop on Reliable Engineering Computing*, Savannah, Georgia, 15-17 September, 2004.

Ang, A., H-S. and Tang, W.H. (1975). Probability Concepts in Engineering Planning and Design, Volume I: Basic Principles. *John Wiley & Sons*.

Arbocz, Johann; and Starnes, James H., Jr.: On a High-Fidelity Hierarchical Approach to Buckling Load Calculations. In "Calladine Festschrift," S. Pellegrino, Ed., Wolters Kluwer Academic Publishers. Dordrecht, The Netherlands, 2002.

Avery, J.L. and B.V. Sankar (2000). Compressive failure of sandwich beams with debonded face-sheets. *Journal of Composite Materials*, Vol. 34, No. 14, pp. 1176-1199.

Grau, D. (2003). Relating Interfacial Fracture Toughness to Core Thickness in Honeycomb-core Sandwich Composites. M.S. Thesis, University of Florida.

Grau, D.L., Qiu, S., Sankar, B.V. (2005) Relation between Interfacial Fracture Toughness and Mode-mixity in Honeycomb Core Sandwich Composites. To appear in Journal of Sandwich Structures & Materials.

Haftka, R.T. (2005). Reflections on Jim Starnes' Technical Contributions. to be presented at the 45th AIAA/ASME/ASCE/AHS/ASC Structures, Structural Dynamics, and Materials Conference, Austin, Texas, 18-21 April 2005.

Kale, A., Acar, E. Haftka, R.T., and Stroud, W.J. (2004). Why Airplanes are so Safe Structurally? Effect of Various Safety Measures on Structural Safety of Aircraft. 45th Structures, Structural Dynamics and Materials Conference, AIAA Paper No. 2004-1629, 19-22 April 2004, Palm Springs California.

Kelton, W.D., Sadowski, R.P. and Sadowski, D.A. (1998). Simulations with Arena. *WCB McGraw Hill*.

Li, Yi-Wei; Elishakoff, Isaac; Starnes, James H., Jr.; and Bushnell, David: Effect of the Thickness Variation and Initial Imperfection on Buckling of Composite Cylindrical Shells: Asymptotic Analysis and Numerical Results by BOSOR4 and PANDA2. International Journal of Solids and Structures, Vol. 34, No. 28, 1997, pp. 3755-3767.

Oberkampf, W. L., DeLand, S. M., Rutherford, B. M., Diegert, K. V. and Alvin, K. F. (1999). A New Methodology for the Estimation of Total Uncertainty in Computational Simulation. AIAA *Non-Deterministic Approaches Forum*, St. Louis, MO, Paper No. 99-1612, April, 1999.

Oberkampf, W.L., Deland, S.M., Rutherford, B.M., Diegert, K.V., and Alvin, K.F. (2000). Estimation of Total Uncertainty in Modeling and Simulation, *Sandia Report* SAND2000-0824, 2000.

Qu, X., Haftka, R.T., Venkataraman, S., and Johnson, T.F. (2003). Deterministic and Reliability-Based Optimization of Composite Laminates for Propellant Tanks. *AIAA Journal*, 41(10), pp. 2029-2036.

Sankar, B.V. and M. Narayanan (2001). Finite Element Analysis of Debonded Sandwich Beams under Axial Compression. *J. Sandwich Structures & Materials*, Vol. 3, No. 3, pp. 197-219.

Suo, Z., (1999), Singularities, interfaces and cracks in dissimilar anisotropic media. *Proc. R. Soc. Lond*. A427, 331-358.